**Proceedings of GT2005:**
**ASME Turbo Expo 2005: Power for Land, Sea and Air**
**June 6-9, 2005, Reno-Tahoe, Nevada, USA**

# GT2005-68463

# THE INFLUENCE OF COMPRESSOR BLADE ROW INTERACTION MODELING ON PERFORMANCE ESTIMATES FROM TIME-ACCURATE, MULTI-STAGE, NAVIER-STOKES SIMULATIONS

**Dale Van Zante**
NASA Glenn Research Center
Cleveland, OH 44135 USA

**Jenping Chen**
Mississippi State University
Mississippi State, MS 39762 USA

**Michael Hathaway**
ARL Vehicle Technology Directorate
Cleveland, OH 44135 USA

**Randall Chriss**
NASA Glenn Research Center
Cleveland, OH 44135 USA

## ABSTRACT

The time-accurate, multi-stage, Navier-Stokes, turbomachinery solver TURBO was used to calculate the aero performance of a 2 1/2 stage, highly-loaded, high-speed, axial compressor. The goals of the research project were to demonstrate completion times for multi-stage, time-accurate simulations that are consistent with inclusion in the design process, and to assess the influence of differing approaches to modeling the effects of blade row interactions on aero performance estimates. Three different simulation setups were used to model blade row interactions: 1.) single passage per blade row with phase lag boundaries, 2.) multiple passages per blade row with phase lag boundaries, and 3.) a periodic sector (1/2 annulus sector). The simulations used identical inlet and exit boundary conditions and identical meshes. To add more blade passages to the domain, the single passage meshes were copied and rotated. This removed any issues of differing mesh topology or mesh density from the following results. The 1/2 annulus simulation utilizing periodic boundary conditions required an order of magnitude less iterations to converge when all three simulations were converged to the same level as assessed by monitoring changes in overall adiabatic efficiency. When using phase lag boundary conditions the need to converge the time history information necessitates more iterations to obtain the same convergence level. In addition to convergence differences, the three simulations gave different overall performance estimates where the 1/2 annulus case was 1.0 point lower in adiabatic efficiency than the single passage phase lag case. The interaction between blade rows in the same frame of reference set up spatial variations of properties in the circumferential direction which are stationary in that reference frame. The phase lag boundary condition formulation will not capture this effect because the blade rows are not moving relative to each other. Thus for simulations of more than two blade rows and strong interactions, a periodic simulation is necessary to estimate the correct aero performance. [*Keywords: blade row interaction, numerical modeling, multi-stage compressor]*

## INTRODUCTION

The NASA Ultra Efficient Engine Technology (UEET) Program is developing and transferring turbine engine propulsion technologies to improve the performance of future aerospace systems. The MSU-TURBO suite of time-accurate, multi-stage, analysis software is a technology being matured and demonstrated by the program. The two stage axial compressor which was designed for the Highly Loaded Light Weight Compressor and Turbine sub-project is used as a test case to demonstrate the computational capability of TURBO. This compressor is referred to as the Proof of Concept Compressor (POCC).

Unsteady Reynolds-Averaged Navier-Stokes (RANS) flow solvers for turbomachinery rotor-stator flows have been under development since the mid-1980s, see for example, Rai [1], Janus & Whitfield [2], Giles [3], Lewis et al. [4], Chen & Whitfield [5], among others. An impediment to the common use of these techniques is the large computational cost of direct

computation of multiple blade-row simulations and rapid turnaround time required, usually within 24 hours, if simulations are to have timely impact on new designs. This requirement limits the routine use of unsteady RANS codes in industrial environment. Fortunately, contemporary computer capability has advanced significantly both in processor speed and memory size concurrently with falling cost since the adoption of high performance parallel computing. TURBO has already proven excellent scalability on parallel systems. One focus of this work is to demonstrate the feasibility of unsteady multi-blade-row turbomachinery simulations with substantial reduction of turnaround time by using the parallel computing power that is now more readily available.

The TURBO code incorporates multiple boundary condition treatments from which the user can choose: phase lag boundary conditions, periodic boundary conditions, and a combination of periodic and phase lag boundaries. All three of the above boundary conditions treatments were evaluated with the POCC test case for numerical efficiency and to ascertain any differences in aeroperformance estimates.

Phase lag boundary conditions are a commonly used practice to reduce computing resources for unsteady simulations without changing the blade count (Erdos and Alzner, [6]). This allows modeling of rotor-stator interaction using only a single blade passage in each blade row. This technique can greatly reduce the computing resources needed for simulations of stages with irreducible blade counts and is useful for time-accurate analyses dominated by unsteadiness at the adjacent blade passing frequency. See Chen and Barter [7] for a detailed description of this modeling technique. The single-stage phase lag capability was implemented in TURBO using a more general approach suitable for simulating multiple stage interaction (Wang & Chen, [8]). Although it generally reduces computing resources in terms of CPUs and memory, direct-storage phase lag simulation typically requires longer computing time to converge the stored history data for the phase lag boundary. In an effort to speed up the convergence performance, a partial frequency mode acceleration technique was implemented to increase the convergence of the phase lag simulations. This method is discussed in more detail later.

While temporal periodicity due to adjacent blade passing can be modeled with the single-passage phase lag modeling, there were concerns over its inability to fully capture the spatial periodicity resulting from interactions of blade rows in the same reference frame, stator-stator or rotor-rotor interactions. These interactions can produce significant circumferential non-uniformities in multi-stage machines [He, et. al., [9]]. This concern is addressed in this study by modifying the single-passage model to use multiple passages in each blade row so that the total circumferential extent of a blade row is always greater than the pitch of the next upstream blade row which is in the same frame of reference. This is an attempt to achieve adequate spatial coverage to capture the incoming wakes while keeping the number of passages computed at a minimum. However, it is recognized that this approach enforces a spatial periodicity that is not necessarily consistent with the spatial periodicity associated with the relative blade counts.

Finally a half-annulus simulation of the entire 2.5-stage machine which captures the inherent periodicity associated with integer multiples of blade counts is also presented in this study. Application of circumferential periodicity models the blade row interactions directly, thereby eliminating concerns over the modeling assumptions in the phase lag simulations and also enforces the correct spatial periodicity. Note however that harmonics that are not associated with integer multiples of shaft frequency, for example stall cells, are improperly constrained to grow at integer multiples of shaft frequency unless a full annulus simulation is done. Since this work is done at the design point for the machine, all temporal harmonics are dominated by shaft speed and a half annulus simulation is sufficient. Although substantially more computing resources are needed, it will be demonstrated that a half-annulus simulation of the 2.5-stage compressor converges much faster than the phase lag simulations. The half-annulus simulation also provides the base-line solution for evaluating the respective merits of the three different approaches, i.e., direct periodicity associated with relative blade counts, single-passage phase lag, and multi-passage phase lag.

What follows is a brief discussion of the TURBO code numerics and recent changes to the code which improved convergence time. Next the setup of the three simulations is discussed followed by the timing and aero performance results. The paper concludes with an analysis of the interactions that lead to the observed differences in aero performance.

## NOMENCLATURE

| | |
|---|---|
| GUI | Graphical User Interface |
| IGV | Inlet Guide Vane |
| POCC | Proof-of-Concept Compressor |
| Pr | Pressure Ratio (Fig 1) |
| R1, R2 | Rotor 1, Rotor 2 |
| S1, S2 | Stator 1, Stator 2 |
| UEET | Ultra Efficient Engine Technology |
| Utip | Tangential tip speed (Fig 1) |
| Wc | Corrected Weight Flow (Fig 1) |
| $\eta$ | Adiabatic efficiency |

## TURBO Numerical Technique

The TURBO code is a 3D, viscous, time-accurate code which solves the Reynolds-averaged Navier-Stokes equations in a rotating cartesian coordinate system. The equations are spatially discretized using a modified upwind scheme (Whitfield, et al. [10]) based on Roe [11] and Osher and Chakravarthy [12]. Temporal discretization is second-order accurate backward differencing. The governing equations are time-marched with an implicit scheme based on iterative Newton algorithm with flux Jacobians computed using the flux-vector splitting technique of Steger and Warming [13] and analytical viscous Jacobians. Matrix inversion is accomplished using a symmetric Gauss-Siedel technique and multiple Newton subiterations are performed at each time step to minimize linearization error. The effects of turbulence are incorporated using a NASA/CMOTT $\kappa$-$\varepsilon$ turbulence model (Zhu and Shi [14]) with wall functions. TURBO computes the flowfields of single or multiple blade passages within either a complete blade row or a periodic circumferential sector of a blade row, and it is capable of simulating unsteady interaction between multiple blade rows using a dynamic sliding interface.

Further information on the numerical aspects of TURBO can be found in Chen and Briley [15].

One goal of the present research is to demonstrate large-scale simulations using parallel computing. It is important that the code is portable across different parallel computing platforms and this was accomplished through use of the Message Passing Interface (MPI) for interprocessor communications. Distributed memory computation is the architectural paradigm of the code, so that each processor (CPU) has exclusive access to its own partition of memory, which typically resides in the processor. The parallel code is implemented by a single-program multiple-data (SPMD) parallelization strategy. In this strategy, a single program is replicated for each processor and run with the data associated with a subdomain of the original computational domain.

The parallel communication framework has been coded to support solution of problems using multi-block structured grids in which the block connectivity of the grid blocks is arbitrary, Chen and Briley [15]. The grids, one per blade passage, need to be partitioned before the execution of the flow solver. The grid partitioning is done with the preprocessor GUMBO (Remotigue [16]), which features a graphical user interface. To reduce the initial transient, an APNASA (Adamczyk [17]) solution (or any 3D RANS solution) can be used to provide initial solutions. This approach has been shown to greatly speed up the convergence of the unsteady simulations (Chen, et.al. [18]).

In addition to the already existing capabilities, two new features have been developed to help improve the turnaround time and are described next.

### Analytical Flux Jacobians

For implicit schemes, flux jacobians are needed to linearize the physical flux vectors, which contain both inviscid and viscous components. The viscous jacobians are computed with a numerical formulation in the older versions of the code. Redundant computation of viscous fluxes had consumed almost one third of the entire computing time. To overcome this problem, an analytical formulation was implemented which resulted in a 30% reduction in CPU time and enhanced code robustness.

### Partial Frequency Mode:

A direct storage method is used in the phase lag simulations (Chen and Barter [7]), which is based on the assumption that passage flow is periodic in time at a prescribed frequency. For embedded blades the unsteady frequency is a combination of the adjacent blade passing frequencies, which in turn depends on the smallest common divisor of their blade counts. With the typical blade counts found in contemporary compressor designs it is common to store a full revolution of phase lag boundary history data. Previous experience indicates the convergence rate of the phase lag simulations is strongly related to the storage size; i.e., the smaller the storage the faster the convergence. To reduce the storage size a modification to the unsteady frequency of each passage is done so that it only accounts for the dominating disturbance from one of the two neighboring blades. For example, in blades where incoming wakes are the dominating disturbances, the phase lag frequency can be temporarily changed to that of the upstream blade passing frequency. The size of the phase lag boundary history data then reduces to only account for the upstream blade count which requires less storage than to account for both upstream and downstream blade counts. This procedure has been shown to be an effective way to move quickly through the initial transient phase when starting from a condition that is far from converged. As the primary periodicity due to the upstream disturbance is established, the downstream disturbance can then be included.

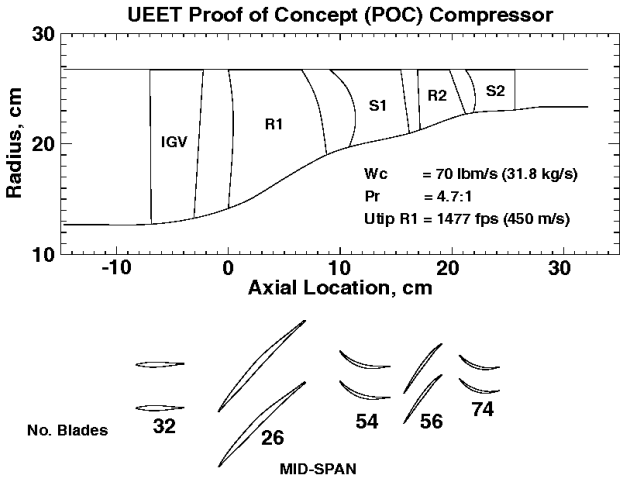


**Figure 1: The UEET 2.5 stage compressor (from Larosiliere, et al. [19]).**

### POCC Test Case

The test case used in this study is the NASA Ultra Efficiency Engine Technology (UEET) Proof of Concept Compressor (POCC). The goal of this design is to demonstrate a highly loaded axial compressor technology capable of delivering 12:1 Pressure Ratio (PR) in four stages with a high level of polytropic efficiency. The POCC compressor, which is the first 2.5 stages of a four stage design, is shown in Figure 1.

## SIMULATION SETUP

### Grid Topology and Inlet/Exit Conditions:

The meshes are one block per blade passage, elliptically smoothed, H-meshes which were produced by the APG code of Beach and Hoffman [20]. They have 80 nodes along the blade chord, 71 points spanwise with 8 cells in the tip/hub clearances packed at the wall, and (except for the IGV) 71 points pitchwise. Mesh size was chosen so that convected features and clearance flows would be adequately modeled based on experience from [21] and [22]. The spacing of the first node off of solid surfaces was consistent with using wall functions ($y^+$ of 15 to 100 with most nodes at 50). GUMBO was used to partition the meshes and to duplicate the meshes for multiple passages per blade row. All three simulations used the identical base meshes. Meshes were simply copied and rotated to create additional passages. The single passage solution contains 3.1M

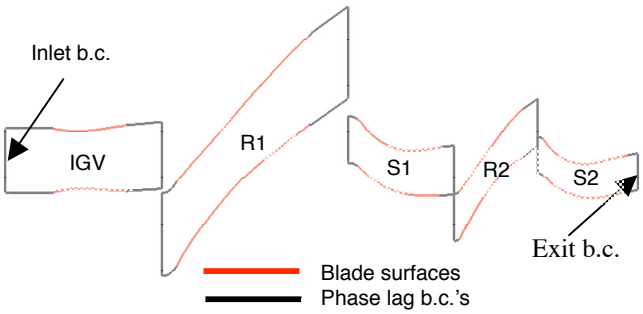


**Figure 2. Case 1: Single-passage phase lag.**

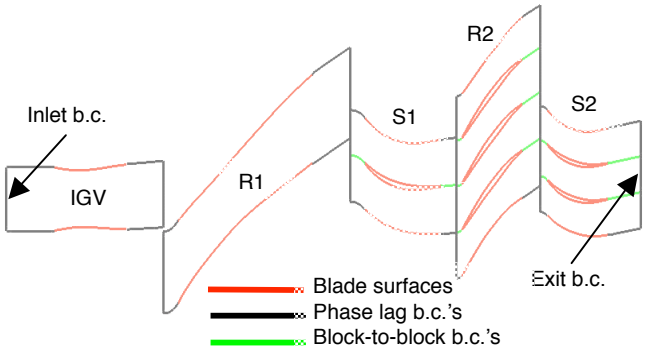


**Figure 3. Case 2: Multi-passage phase lag.**

nodes, the multi passage 6.9M nodes and the half annulus solution 76.4M nodes.

Early in this research project the computational resources available were only adequate for the single and multi passage cases. Thus, a modification to Stator 2 blade count from 74 to 75 was made to the single and multiple passage simulations to keep the computational resources for the multiple passage simulation manageable. The blade count change was only done to allow the comparison of the single and multiple passage simulations. The single passage phase lag simulation has no inherent restriction on blade count. The addition of a single Stator 2 blade was done without rescaling the blade chord or changing the axial spacing. An APNASA simulation of the POCC showed < 0.1 point change in adiabatic efficiency due to the blade count change.

1D non-reflecting inlet and exit conditions were used with the base flow derived from an APNASA solution. These 1D boundary conditions were derived from small perturbation theory to allow the base flow to adjust as the flow inside the computational domain evolves (Chen et al. [18]). The same inlet and exit conditions were used for all three simulations. The history data time extent for each blade row is set by the user within the constraints that it must be consistent with the temporal periodicity as determined by the relative blade counts. Because of blade counts, the longest time history record of the five blade rows is for Rotor 2, 1/3 revolution for the single passage case and 1 revolution for the multi passage case. The influence of this time history record length is discussed further in the simulation convergence section.

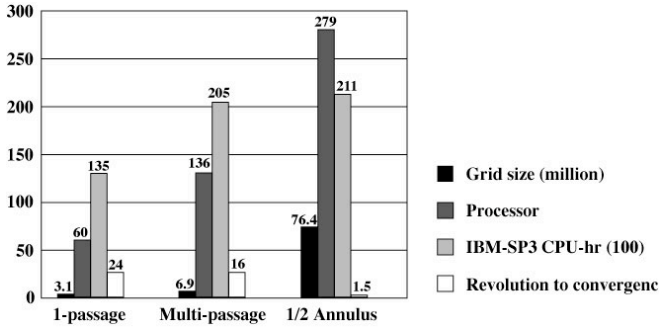


**Figure 4. Computer resources used.**

**Case 1: Single-passage Phase lag**

The standard phase lag modeling is used in this case in which only one blade passage is computed for each blade row. This technique uses the least amount of computer resources and therefore allows smaller grid size per processor to reduce computing time. The phase lag boundary conditions were applied at the circumferential interface between blade passages as indicated in Figure 2 and the sliding interface between blade rows.

With approximately 50K grid nodes per processor, the simulation used 60 processors. The unsteady frequency for each blade row is a combination of the blade passing frequencies of the two adjacent blade rows.

**Case 2: Multiple-passage Phase lag:**

While temporal periodicity arising from adjacent blade rows can be modeled with the single-passage phase lag simulations, the spatial periodicity from upstream blade rows in the same reference frame cannot. A different simulation methodology is proposed here to examine the importance of this effect. Multiple passages are used in each blade row so the spatial coverage of a particular blade row is always greater than the pitch of the next upstream blade row in the same frame of reference. It was hoped that the increased circumferential extent of the domain would better capture the rotor-rotor and stator-stator interactions while keeping the number of passages computed at a minimum. The single passage mesh in each blade row was duplicated such that the total spatial content covers one complete passage of the blades two blade rows upstream. The modified geometry resulted in the computation of 11 passages with 1-1-2-4-3 blade count as shown in Figure 3.

The multiple passages within each blade row form a group where phase lag boundary conditions can be applied at the outer boundaries. Note this enforces a spatial periodicity that is inconsistent with the actual spatial periodicity (i.e., two stator 1 passages do not allow an integer multiple of IGV passages). Block-to-block interface communication was applied to passage interfaces within the group. For interfaces between blade rows the sliding interface was used. 136 processors were used with approximately 50K grid nodes per processor.

**Case 3: Periodic Sector Simulation (half annulus):**

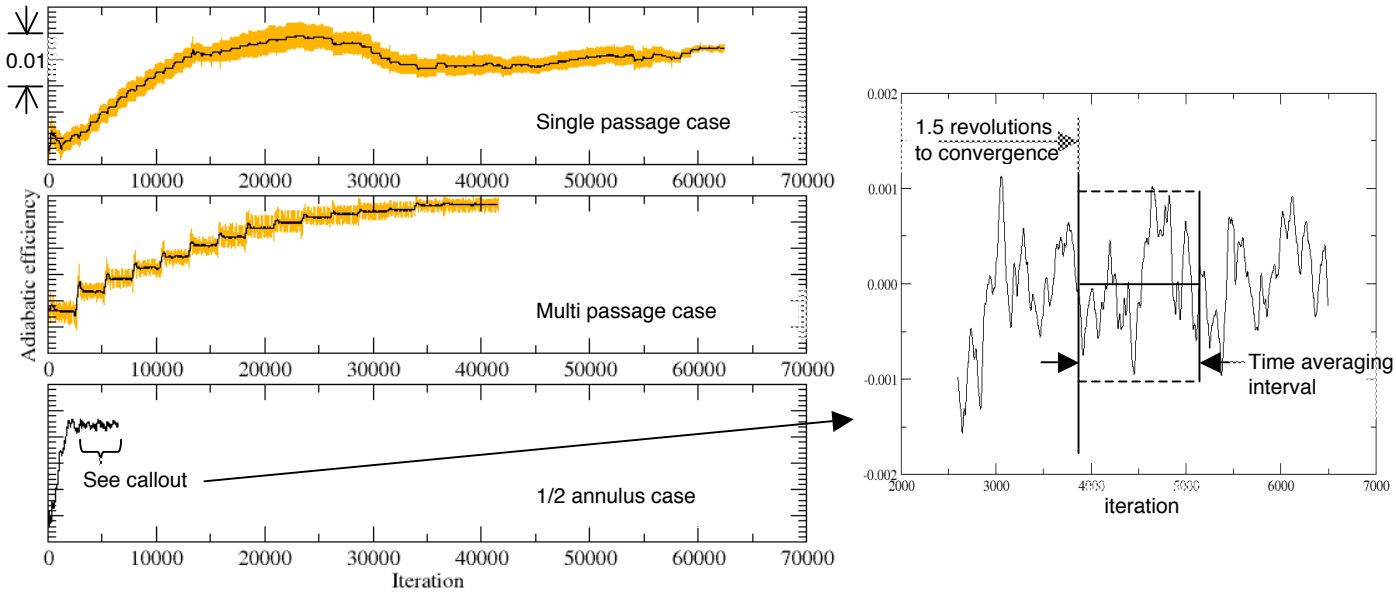


**Figure 5. Adiabatic efficiency convergence history. (0.01= 1 point)**

The assumption of phase lag periodicity is valid only when the unsteady flow frequencies are multiples of neighboring blade passing frequency. Although it generally reduces computing resources in terms of CPUs and memory, phase lag simulation typically requires longer computing time because of the need to converge the history data in addition to the questions raised above as to the resolution of the spatial periodicity being adequately accounted for in multi-stage environments. Direct application of periodicity models physics directly, hence providing more trusted simulations.

The blade count (32-26-54-56-74) of this geometry allows for the periodic simulation to compute one half annulus (16-13-27-28-37) of the entire 5-blade-row compressor with circumferential periodicity. Dynamic sliding interface is applied between blade rows for time-accurate blade interactions. This simulation used 279 processors with approximately 270K nodes per processor. The periodic simulation uses the least modeling assumptions and therefore will be used as the baseline result for comparison in this study.

## RESULTS

### Computing Resources Required:

An IBM SP3 system was used for the POCC simulations. Computer resources for each case are shown in Figure 4 in terms of CPUs and time. The overall resource requirements can be expressed in total CPU-hrs used for the simulation (number of processors multiplied by time used). The half annulus simulation seemed to provide the best return on investment as it produces the highest fidelity (least assumptions) result with only a small increase in total CPU-hrs. If the number of CPUs is a constraint, the single-passage phase lag simulation provides the most viable means to conduct the unsteady simulation.

### Simulation Convergence:

Simulation convergence was determined by monitoring adiabatic efficiency from the TURBO performance history file. Adiabatic efficiency is computed at each iteration from mass average properties at the exit of the computational domain. The convergence of adiabatic efficiency is slower than mass flow or pressure ratio and thus represents a stringent test of convergence. All three simulations were started from equivalent three dimensional base flows. Figure 5 shows the convergence history for the three simulations. Convergence of the 1/2 annulus simulation is considered first.

The 1/2 annulus case was considered converged when the instantaneous value of efficiency was +/- 0.1 point from the mean computed over 1/2 revolution (1300 iterations):

$$\max\left|\eta(t)-\overline{\eta}\right| \le 0.1 \text{ point}$$

$$\text{where } \overline{\eta} = \frac{1}{T}\int_{t}^{t+T} \eta dt, \mathrm{T} = 1300 \text{ iterations}$$

See the callout of Figure 5 for a graphical illustration of this. The simulation was considered converged at 1.5 rotor revolutions but was run for a total of 2.5 revolutions to be certain. The convection time from inlet to exit of the computational domain is 0.5 revolutions. Pressure wave propagation time is 0.2 revolutions downstream and 0.5 revolutions upstream going. It is reasonable to assume that adequate convection/propagation transit times have occurred for simulation convergence especially since the initial base flow state is close to the converged time accurate flow state.

The efficiency history of the phase lag simulations must be analyzed differently than that of a periodic simulation because the phase lag computational domain does not encompass a spatially periodic sector. This leads to 'fuzz' in the convergence history (shown in orange in Figure 5) that is a product of the limited circumferential domain over which the average properties are determined. Additionally the phase lag time

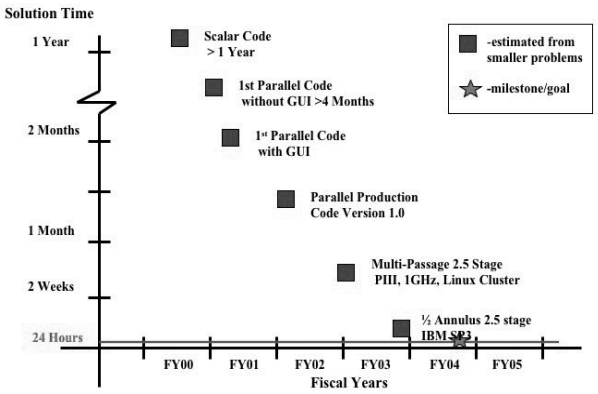


**Figure 6. Time to complete solution for 2.5 stage compressor.**

history has a record length which is set by the user, for example, one revolution or 2600 iterations is the maximum record length needed for the multi passage case. TURBO uses a direct storage method where the time history is updated by averaging the instantaneous values at the boundary with previously stored values. Once the entire record length is updated the process starts again at the beginning of the record. This leads to a step change in efficiency and thus convergence is quantized by time history record length in that the user must wait for the next pass through the time history to ascertain if the efficiency value remains within the tolerance band and if the trend is stable.

This process is best illustrated by the multi passage case shown in Figure 5. The orange line is the performance history directly from TURBO. The black line is a running average mean and shows the step changes in efficiency due to the time history record length. The changes in mean efficiency become smaller from revolution to revolution until the change is smaller than 0.1 point for two consecutive revolutions.

The single-passage case required 24 revolutions, the multiple-passage case required 16 revolutions, and the periodic case 1.5 revolutions to converge. Even though more computing resources are needed for the half annulus periodic simulation, the convergence speed is at least one order of magnitude faster than the phase lag simulations as shown by Figure 5.

**Simulation Turnaround Time:**

Hardware improvement is a major factor in realizing the fast turnaround. TURBO has been used on computers based on 800 MHz Pentium II processors for Linux clusters to 1.3 GHz Power 4 processors for the IBM P4 supercomputer. The scalable parallel architecture of TURBO is able to utilize these improved hardware capabilities as they become available. In view of the hardware advances, as shown in Figure 6, the combination of hardware and software improvements has resulted in at least two orders of magnitude reduction in turnaround time over the past five years in addressing problems as large as the POCC case. The computation time is decreasing even as the size of the simulation increases during the evolution of the TURBO code. The move from scalar to parallel code architecture resulted in both reduced solution times and also the ability to compute larger problems. The addition of a GUI

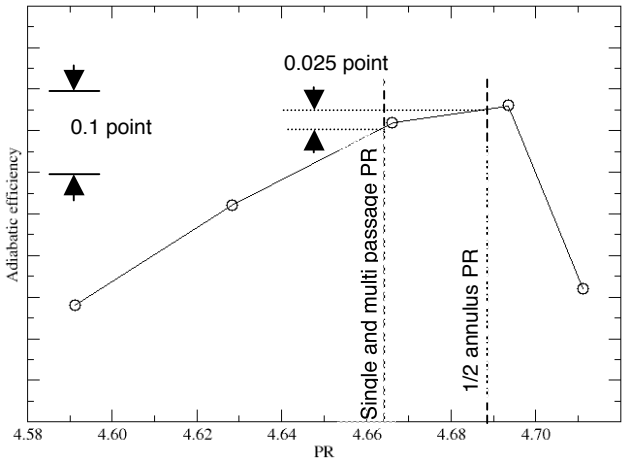


**Figure 7. Efficiency versus pressure ratio characteristic from APNASA.**

greatly simplified solution setup. Unsteady simulations of the entire compression system using RANS techniques are now within reach of current computing capacity. The demonstration of 24 hour turnaround time was a UEET program milestone. The 24 hour turnaround is based on timing studies done with the IBM P4.

**Aero performance estimates:**

To determine overall performance the simulations must be appropriately time and spatially averaged. The performance calculation method used for results presented here is explained in detail in Appendix A. The aerodynamic performance estimates from the three simulations are summarized in Table 1.

Table 1. Overall performance results.

| | Mass flow, (kg/s) | Total Pressure Ratio, Pt/Pref | Adiabatic Efficiency, 0.01= 1 point |
|---|---|---|---|
| Single passage phase lag | 32.24 | -0.03 | +0.010 |
| Multi passage phase lag | 32.23 | -0.03 | +0.006 |
| 1/2 annulus | 32.24 | Baseline | Baseline |

The simulations converged to identical mass flow but showed a small difference in pressure ratio and a 1.0 point maximum difference in adiabatic efficiency. Mass flow is not a good indicator of operating point, since this compressor has a nearly vertical design speed characteristic. The APNASA code has been used to generate the design speed line and the efficiency versus pressure ratio relationship obtained, Figure 7. With the 1/2 annulus simulation as a baseline, the single and multi passage simulation efficiencies can be adjusted based on their difference in pressure ratio from baseline. The adjustment is negligible being only 0.025 points in efficiency for both simulations. This indicates that the differences in efficiency are

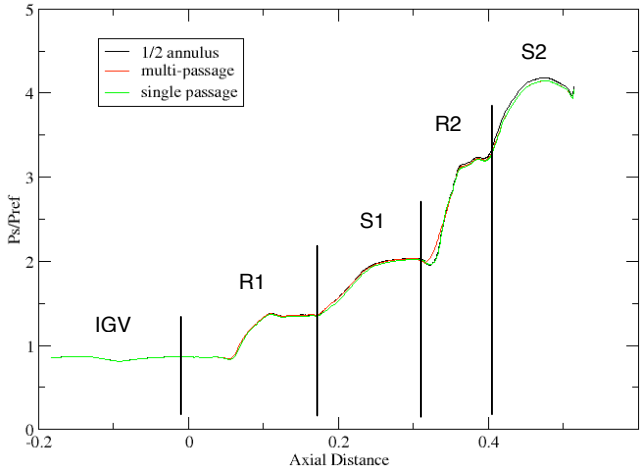


**Figure 8. Axisymmetric static pressure on the POCC casing.**

a result of differences in modeling and not due to a change in operating point.

## DISCUSSION

A more detailed analysis of the three simulations is undertaken to establish a possible cause of the differing overall adiabatic efficiencies. The work of He [9] notes that phase lag boundary conditions will not capture the effects of rotor-rotor and stator-stator interactions because these interactions are stationary in the reference frame of a blade row. These interactions lead to circumferential flow field variations and differing passage to passage time average flow fields. He illustrates what he calls 'aperiodic efficiency' variations of 0.65 point in polytropic efficiency at the exit of a rotor row. Similar passage to passage variations in time average flow were observed when studying the POCC flows in detail. For example, Figure 13 in Appendix A illustrates the passage to passage differences in the Rotor 2 shock structure due to the circumferentially nonuniform inlet conditions to the rotor.

It should be noted that the mechanism that creates the circumferential variations described in this work differs from that described in Shang, et. al. [23]. Their work involved a single stage machine where the local back pressure effect of the stator caused a change in rotor loss production. Thus flow into the stator had non uniform circumferential properties due to the change in rotor loss. This is an 'unsteady' effect and differs from rotor-rotor or stator-stator interactions.

The degree of blade row coupling will determine the amplitude of the passage to passage variation and thus the impact of the modeling methodology on the overall performance results. Before looking at the details of the passage to passage variations it is useful to look at the overall matching of the machine.

### Overall compressor matching:

Figure 8 shows the axisymmetric average static pressure on the casing for the three TURBO cases to compare pressure rise and mean rotor shock locations. The differences in static pressure rise between the simulations are very small and the rotor shock structure is the same in all. The pressure rise differences between simulations occur gradually with axial distance through the machine and no large change in matching/performance for an individual blade row is noticeable. The effects of the different simulation methodologies appear to be subtle and cumulative through the machine.

### Circumferential variations of time average properties

The three simulations were completed using different modeling methods but careful attention to maintain identical grid topology and identical inlet and exit boundary conditions. Time unsteady features are modeled by direct periodicity or phase lag boundary conditions with the more general formulation of phase lag boundary capable of simulating the multiple frequencies present for an embedded blade row. Thus, assuming that the time unsteady character of all simulations is essentially equivalent, the feature that differentiates the simulations from each other is the ability of the modeling assumptions to capture the spatial non-uniformities.

As shown by He [9] and reconfirmed for the results shown here, efficiency and entropy show equivalent trends for circumferential non-uniformities. Because it is more intuitive, efficiency will be used in the following analysis.

Using the time average state variables the adiabatic efficiency was calculated near the Rotor 1/Stator 1 mesh interface in the Stator 1 flow field (absolute frame) for the half annulus solution, Figure 9. The figure shows significant variation of adiabatic efficiency with circumferential position. For a more quantitative view the adiabatic efficiency with the mean value removed is plotted along the 50% span line, Figure 10a.

In Figure 10a the peak to peak amplitude of the efficiency variation is nearly 1.0 point. The primary spatial period seen corresponds to the IGV spacing which would be expected as Rotor 1 processes the IGV wakes. However, several other longer and shorter spatial periods are also present. Following the ideas of Williams [24] a spatial FFT is done to better understand circumferential wave number content and contribution, see Figure 10b.

Figure 10b shows the IGV (circumferential wave number 32) to be the primary contributor to the circumferential variation. However, modes corresponding to the Stator 1 first (circumferential wave number 54), second (circumferential wave number 108), and third (circumferential wave number 162) harmonics have peaks within an order of magnitude of the IGV mode. Beat modes of sums and differences (circumferential wave numbers 76 and 86) are also readily apparent which indicates an interaction between the IGV and Stator 1.

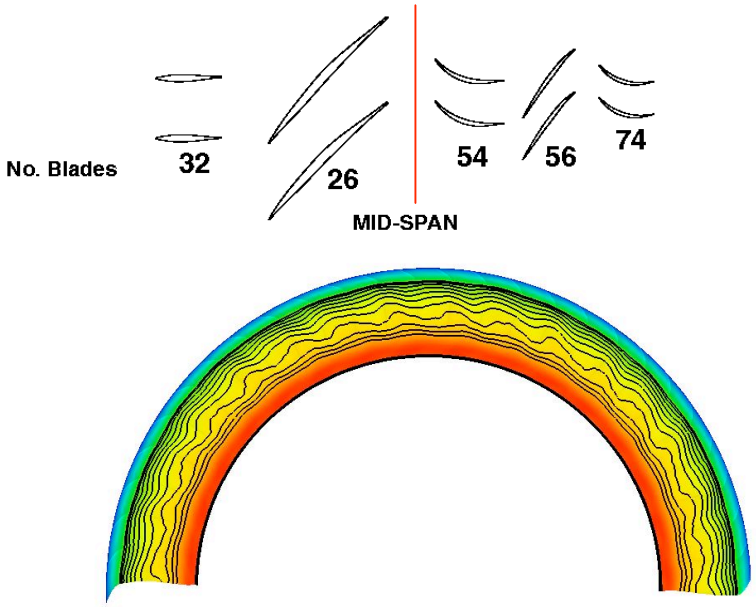


**Figure 9: Adiabatic efficiency at the inlet plane of the Stator 1 mesh, 1/2 annulus solution. Contour lines increments are 1 point in efficiency.**

The 1/2 annulus simulation encompasses the correct periodic spatial extent and thus results from the simulation will contain all the correct coupling for rotor-rotor and stator-stator interactions. As seen in Figures 10a and 10b the inflow to stator 1 has a circumferential structure that is relatively complex in terms of the circumferential wave number content due to IGV-stator interaction. This will also be true of the inflow to Rotor 2 and Stator 2. The spatial non-uniformities will drive subtle but cumulative changes in aero performance through the machine.

The cases using phase lag boundaries will not completely capture the stator/stator or rotor/rotor interactions due to the limited circumferential extent of the computation domain. A representation of 1/2 the compressor annulus can be recreated from phase lag simulation results by a post-processing procedure which is based on the phase lag methodology. This was done for the single and multi passage cases. The adiabatic efficiency profiles from 50% span Stator 1 inlet were extracted and are shown in Figures 11a and 12a. It is evident that the circumferential wave number content is substantially different from the 1/2 annulus case. Note that at this highly magnified scale the mean is non-stationary. This is the result of applying phase lag boundary conditions in a flow field that has spatial circumferential non-uniformities.

Spatial FFTs of the single and multi passage efficiency profiles are shown in Figures 11b and 12b. The circumferential wave number content of the single passage case, Figure 12b, is almost entirely composed of Stator 1 content and harmonics. The IGV wave number content is more than an order of magnitude lower than the Stator 1 peaks. In this case the circumferential extent of the Stator 1 domain is much smaller ($1/27^{th}$) than the 1/2 annulus periodic sector and is not able to capture the IGV-Stator 1 interaction. This results in a 'spatial filtering' of the information that is passed between blade rows and will occur for Rotor 2 and Stator 2 as well.

The intent of the multi passage case was to include a greater circumferential domain to better capture the IGV-Stator interaction. As shown by the circumferential wave number content in Figure 11b, the results are somewhat improved over the single passage case. There is now some IGV content as indicated by the larger amplitude at circumferential wave number 32 although the peak is smeared over several wave numbers. The results appear to be strongly influenced by the spatial extent used in the calculation. Note the two Stator 1 pitch period present in Figure 11a. The multi passage case has captured some of the IGV-Stator 1 interaction as evidenced by increased IGV wave number content but does not contain the beat wave numbers which would indicate a true coupling of the IGV and stator.

The 1/2 annulus simulation case results includes the blade row coupling present in the POCC. An analysis of the blade row coupling present in the single and multi passage cases is consistent with the comparisons of overall performance. That is, the greatest difference in circumferential wave number content and thus largest filtering of information occurs between the single passage and 1/2 annulus cases which is consistent with the largest difference in overall performance. Adding additional circumferential extent to the computational domain in the multi passage case improved the circumferential wave number content somewhat and brought the overall performance estimates into better agreement with the 1/2 annulus case.

## CONCLUSIONS:

A 2.5 stage compressor has been simulated with the time-accurate, multi stage, turbomachinery solver TURBO using three different modeling strategies: single passage per blade

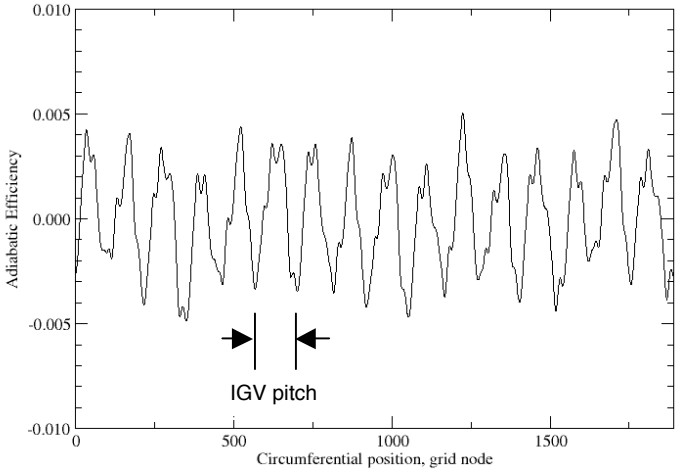


**Figure 10a. Circumferential variation of adiabatic efficiency at 50% span, Stator 1 inlet plane for the 1/2 annulus solution (average value has been removed).**

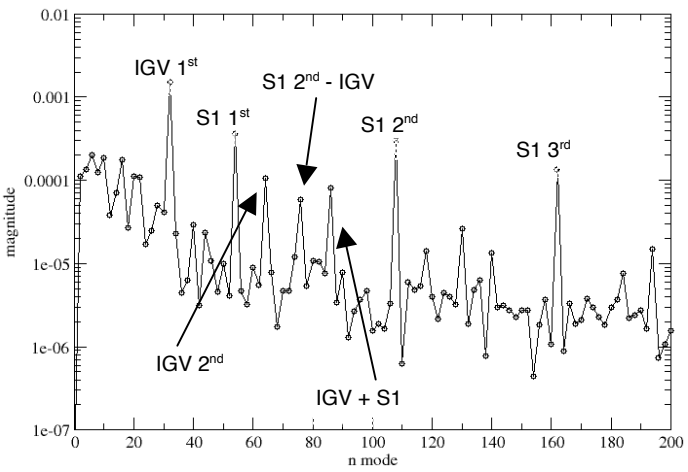


**Figure 10b. Modes present in the 1/2 annulus solution.**

row with phase lag boundary conditions, multiple passages per blade row with phase lag boundary conditions, and a 1/2 annulus sector. The simulations all used identical meshes and inlet/exit boundary conditions. Major findings are as follows:

1. The 1/2 annulus simulation converged an order of magnitude faster than the simulations which incorporated phase lag boundary conditions. Even though the computer resources requirements are large in terms of the number of processors for the 1/2 annulus simulation, the actual computing time for which the resources are required is small. The 1/2 annulus simulation is then competitive with the phase lag simulations when considered on a combined resource-time basis.
2. Different modeling strategies employed in the simulations resulted in different overall adiabatic efficiency predicted with the greatest difference of 1.0 points between the single passage case and the 1/2 annulus simulation.
3. The 1/2 annulus simulations shows substantial circumferential variation of thermodynamic properties at the Stator 1 inlet plane due to interactions of blade rows in the same frame of reference. This will be true of Rotor 2 and Stator 2 as well. Simulations using the phase lag boundary conditions were not able to completely capture this effect even with multiple passages per blade row. The consequence of this information filtering is a subtle and cumulative change in performance through the machine as shown by the differences in overall performance.

## ACKNOWLEDGMENTS

The authors would like to thank Tony Strazisar and John Adamczyk for many useful comments and discussions, Chuck Niggley of NAS for computing resources, and the Naval Oceanographic Major Shared Resource Center for computing resources. Thanks to Mark Turner for assistance with axisymmetric averaging tools for general meshes with acknowledgement to Lyle Dailey as the primary tool developer. Support for Jenping Chen is from NASA contract NAS3-00181, Eric McFarland, Contract Monitor. His support is gratefully acknowledged. This work was supported by the NASA Ultra Efficient Engine Technology Program.

## REFERENCES

1. Rai, M. M., "Navier-Stokes Simulations of Rotor/Stator Interactions Using Patched and Overset Grids," AIAA J. Propulsion and Power, 3(5), 1986, pp. 387-396.

2. Janus, J.M. and Whitfield, D. L., "A Simple Time-Accurate Turbomachinery Algorithm with Numerical Solutions of an Uneven Blade Count Configuration," AIAA-89-0206, January 1989.

3. Giles, M.B., "Stator/Rotor Interaction in a Transonic Turbine," AIAA-88-3093, 1988.

4. Lewis, J.P., Delaney, R. A., and Hall, E. J., "Numerical Prediction of Turbine Vane-Blade Aerodynamic Interaction," ASME J. Turbomachinery, 111, 1989, pp. 387-396.

5. Chen, J.P., and Whitfield D.L., ``Navier-Stokes Calculations for the Unsteady Flowfield of Turbomachinery", AIAA-93-0676, Reno, January 1993.

6. Erdos, J.I., Alzner, E., and McNally W., "Numerical Solution of Periodic Transonic Flow Through a Fan Stage," AIAA Journal 15 (11), pp1559-1568, 1977.

7. Chen, J.P., Barter, J.W., "Comparison of Time-Accurate Calculations for the Unsteady Interaction in Turbomachinery Stage," AIAA 98-3292, July 1998.

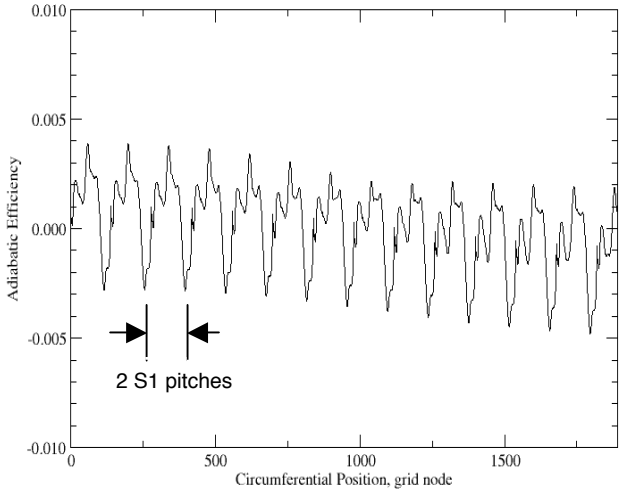


**Figure 11a. Adiabatic efficiency at 50% span, Stator 1 inlet for the multi-passage case.**

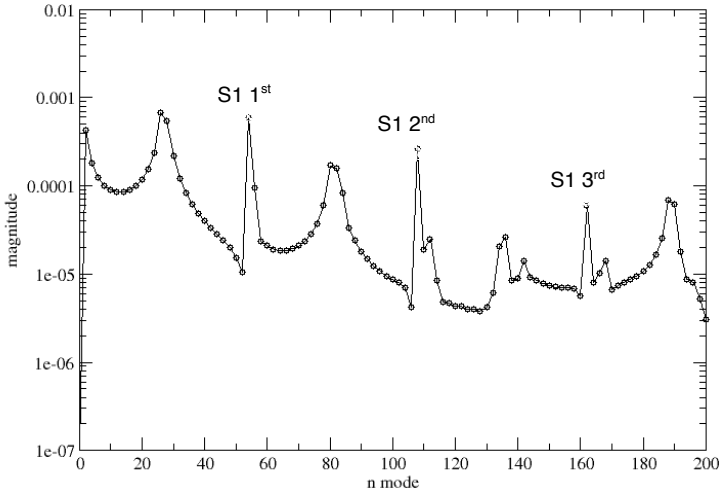


**Figure 11b. Modes present in the multi-passage case.**

8. Wang, X., Chen, J.P., "A Post-Processor to Render Turbomachinery Simulations," AIAA-2004-615, Jan. 2004.

9. He, L., Chen, T., Wells, R.G., Li, Y.S., and Ning, W., "Analysis of Rotor-Rotor and Stator-Stator Interferences in Multi-Stage Turbomachines," ASME Journal of Turbomachinery, Vol. 124, pp. 564-571, October 2002.

10. Whitfield, D. L., Janus, J. M., and Simpson, L. B., 1988, "Implicit Finite Volume High Resolution Wave-Split Scheme for Solving the Unsteady Three-Dimensional Euler and Navier-Stokes Equations on Stationary or Dynamic Grids," MSSU-EIRS-ASE-88-2.

11. Roe, P. L., 1981, "Approximate Riemann Solvers, Parameter Vectors, and Difference Schemes," Journal of Computational Physics, Vol. 43, pp. 357-372.

12. Osher, S., and Chakravarthy, S. R., 1984, "Very High Order Accurate TVD Schemes," ICASE Report No. 84-44.

13. Steger, J. L., and Warming, R. F., 1981, "Flux Vector Splitting of the Inviscid Gasdynamic Equations with Application to Finite-Difference Methods," Journal of Computational Physics, Vol. 40, pp.263-293.

14. Zhu J. and Shih, T.-H., "CMOTT Turbulence Module for NPARC," NASA CR 204143, Aug. 1997.

15. Chen, J.P., and Briley W.R., "A Parallel Flow Solver for Unsteady Multiple Bladerow Turbomachinery Simulations," ASME-2001-GT-0348. June 2001, New Orleans, LA.

16. Remotigue, M.G., "Structured Grid Technology to Enable Flow Simulation in an Integrated System Environment," PhD Dissertation, Mississippi State University, Dec. 1999.

17. Adamczyk, J.J., "Model Equation for Simulating flow in Multistage Turbomachinery," ASME 85-GT-226. 1984.

18. Chen, J. P., Celestina, M., and Adamczyk, J.J., "A new Procedure for Simulating Unsteady Flows Through Turbomachinery Blade Passage," ASME-94-GT-151, 1994.

19. Larosiliere, Louis, Wood, Jerry R., Hathaway, Michael D., Medd, Adam J., and Dang, Thong Q., "Aerodynamic Design Study of Advanced Multistage Axial Compressor," NASA TP-2002-211568, December 2002.

20. Beach, T.A. and Hoffman, G., "IGB Grid: User's Manual (A Turbomachinery Grid Generation Code)," NASA Contractor Report 189104, January 1992.

21. Van Zante, D.E., Strazisar, A.J., Wood, J.R., Hathaway, M.D., and Okiishi, T.H., "Recommendations for Achieving Accurate Numerical Simulation of Tip Clearance Flows in Transonic Compressor Rotors," Journal of Turbomachinery, Vol. 122, October 2000, pp. 733-742.

22. Van Zante, D.E., To, Wai-Ming, and Chen, Jen-Ping, "Blade Row Interaction Effects on the Performance of a Moderately Loaded NASA Transonic Compressor Stage," ASME GT2002-30575, June 2002, Amsterdam, The Netherlands.

23. Shang, T, Epstein, A H, Giles, M B, and Sehra, A K, "Blade Row Interaction Effects on Compressor Measurements," Journal of Propulsion and Power, Vol. 9, No. 4, 1993.

24. Williams, M.C., "Inter and Intrablade Row Laser Velocimetry Studies of Gas Turbine Compressor Flows," ASME Journal of Turbomachinery, Vol. 110, pp. 369-376, July 1988.

25. Denton, J D and Cumpsty, N A, "Loss Mechanisms in Turbomachines," IMechE, 1987.

26. Kronauer, Richard and Grant, Howard, "Pressure Probe Response in Fluctuating Flow," Proceedings of the 2cd US

 

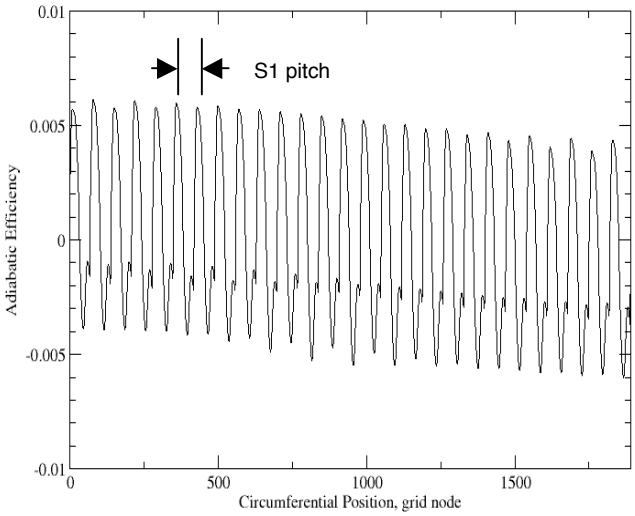


**Figure 12a. Adiabatic efficiency at 50% span, Stator 1 inlet for the single-passage case.**

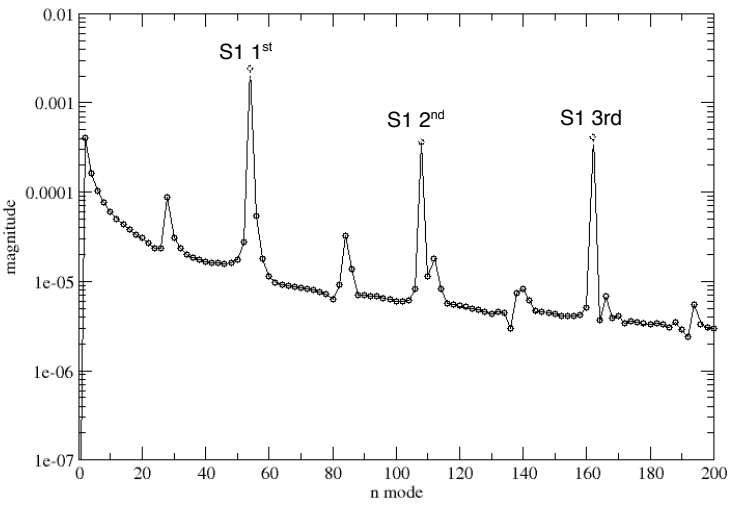


**Figure 12b. Modes present in the single-passage case.**

National Congress of Applied Mechanics, Ann Arbor, Michigan, June, 1954.

## APPENDIX A: COMPUTATION OF LOSSES IN UNSTEADY FLOWS

The only accurate measure of loss in an unsteady flow is entropy (Denton and Cumpsty [25]). However entropy cannot be measured directly in an experiment, but is instead inferred by measurements of total pressure and total temperature. In multistage compressors these interstage measurements of total pressure and total temperature are typically done using stator leading edge instrumentation. Overall performance might be determined by rake measurements downstream of the last blade row. The stator leading edge instrumentation is in an especially unsteady flowfield and is thought to, at best, measure an approximation of the time average total pressure and total temperature (Kronauer and Grant [26]).

On the other hand, from a numerical simulation there are several possible methods of computing loss or efficiency, although not all methods are consistent with what the experimental instrumentation is believed to be measuring. TURBO has a time averaging routine which runs concurrently with the flow solver and averages the code's state variables, (ρ,ρu,ρv,ρw,ρe). This is convenient for the user since time averaging is no longer a post-processing step and file storage requirements are minimized. However, total pressure and total temperature (and thus adiabatic efficiency) are non-linear functions of the state variables and thus:

$$\eta\left(\overline{P}_T, \overline{T}_T\right) \neq \eta\left(\overline{\rho}, \overline{\rho u}, \overline{\rho v}, \overline{\rho w}, \overline{\rho e}\right)$$

for an unsteady flow. But estimating the efficiency based on time average state variables may be satisfactory if the efficiency calculation locations are chosen judiciously in areas of relatively low unsteadiness.

To determine the magnitude of this inequality, the time averaging routine of TURBO was modified to output both time averages of the state variables but also time averages of pressure, total pressure, total temperature, mass-weighted total temperature, and mass-weighted entropy. The multi-passage simulation was time averaged with the modified routine.

Using the modified time average results, adiabatic efficiency was calculated by three different methods: 1.) using total temperature and total pressure calculated from the time average state variables, 2.) using time average total pressure and total temperature, 3.) using the time average mass-weighted total temperature and entropy to calculate total pressure and then adiabatic efficiency. Time average total pressure and total temperature are used so that the analysis is consistent with what is measured experimentally. Calculation 3 represents a thermodynamically rigorous but experimentally unrealizable method to determine efficiency. It is included for completeness.

The difference in the efficiency values is shown on a 50% span surface for Stator 1, Rotor 2, and Stator 2 in figure 13 for calculation 2 versus 1 and Figure 14 for calculation 3 versus 1.

The rating plane for the compressor is the stator 2 exit plane. The maximum error at the downstream overall performance rating plane for the compressor is less than 0.1 points. Any of the calculation methods would give an estimate of overall performance to within engineering accuracy.

Additionally the largest errors occur for all blade rows in their central spans where narrow wakes and shocks are present. In the endwalls the relative unsteadiness is much lower because, for instance, the rotor tip clearance flow and the rotor wake fill nearly the entire blade pitch and are seen as a quasi-steady flow by the following blade row.

For the inlet region of embedded Stator 1, the error associated with calculating efficiency based on time average state variables is 0.2 to 0.4 points depending on circumferential location. Errors downstream of Stator 1 exceed 1 point in efficiency due to the presence of the bow shock from the transonic Rotor 2. Note that the Stator 1 exit performance could be determined with less error by using the Rotor 2 solution where the bow shock is essentially steady in the rotor frame of reference.

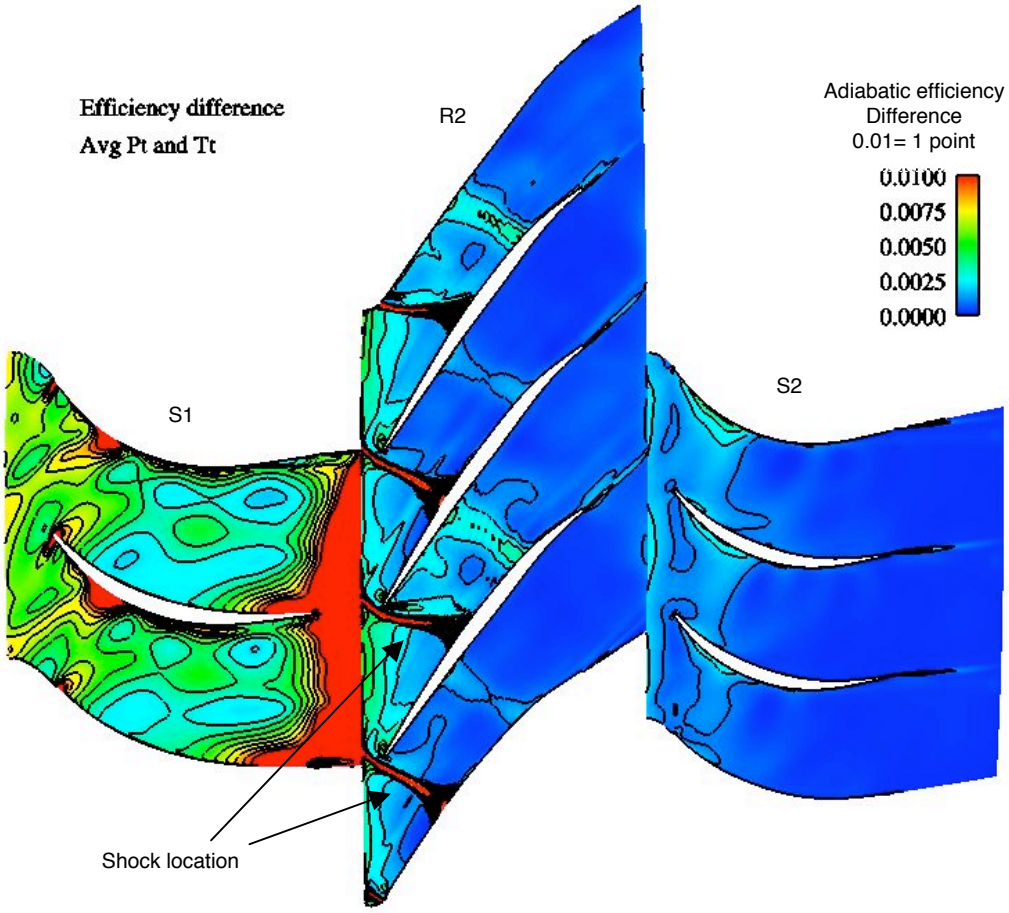


**Figure 13. Difference in adiabatic efficiency from a calculation using time average total temperature and total pressure and a calculation using time average state variables.**

In summary, relative comparisons of efficiency at the same spatial location between the three simulations are valid. Comparison of absolute values is only valid if the errors at that spatial location are low. The entrance to Stator 1 and the rating plane downstream of Stator 2 are examples of locations where the time average state variables can be used to calculated performance to within engineering accuracy. With the above limitations noted, the analysis contained in this paper is based on the time average state variables.

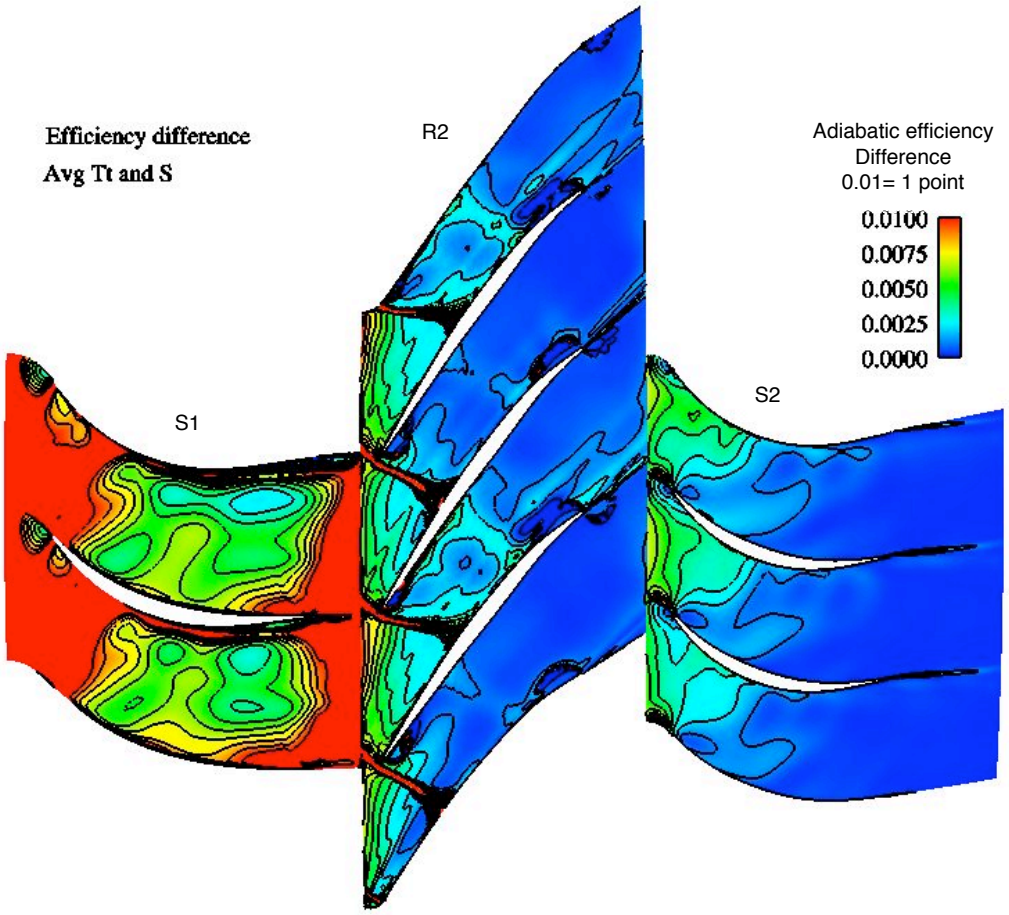


**Figure 14. Difference in adiabatic efficiency from a calculation using mass weighted time average total temperature and total pressure from mass weighted entropy and a calculation using time average state variables.**